Temperature-dependent valence state within the metallic phase of BaV$_{10}$O$_{15}$ probed by hard x-ray photoelectron spectroscopy

S. Dash,[1] M. Okawa,[2] T. Kajita,[3] T. Yoshino,[1] R. Shimoyama,[2] K. Takahashi,[2] Y. Takahashi,[2] R. Takayanagi,[2] T. Saitoh,[2] A. Yasui,[4] E. Ikenaga,[5] N. L. Saini,[6] T. Katsufuji,[3] and T. Mizokawa[1]

[1]*Department of Applied Physics, Waseda University, Shinjuku, Tokyo 169-8555, Japan*
[2]*Department of Applied Physics, Tokyo University of Science, Katsushika, Tokyo 125-8585, Japan*
[3]*Department of Physics, Waseda University, Shinjuku, Tokyo 169-8555, Japan*
[4]*Japan Synchrotron Radiation Research Institute, Sayo, Hyogo 679-5198, Japan*
[5]*Institute of Materials and Systems for Sustainability, Nagoya University, Nagoya 464-8603, Japan*
[6]*Department of Physics, University of Roma "La Sapienza" Piazalle Aldo Moro 2, 00185 Roma, Italy*

We have studied electronic properties of BaV$_{10}$O$_{15}$ in the intermediate-temperature phase as well as in the high-temperature metallic phase by using hard x-ray photoemission spectroscopy (HAXPES). The V $2p$ HAXPES show a shift in the high-temperature phase between 300 and 245 K which is similar to the shift of spectral weight near the Fermi edge. The binding energy of the O $1s$ HAXPES peak does not change except a slight shift of the lower binding energy edge in the opposite direction between 300 and 180 K across the transition to the intermediate-temperature phase. This behavior is in sharp contrast to the transition to the low-temperature insulating phase where V $2p$ and O $1s$ HAXPES show dramatic shifts in the same direction. This indicates that the charge-orbital change in the intermediate-temperature phase is driven by the correlated V $3d$ electrons and is electronic. The V$^{2.5+}$-V$^{2.5+}$ bond ordering is related to the metallic contribution and gradually decreases with cooling from 300 K. The valence-band HAXPES show the metallic features of the pseudogap behavior near the Fermi edge in and above the intermediate-temperature phase due to V$^{2.5+}$-V^{3+} charge fluctuation. The magnitude of the pseudogap increases from 300 to 180 K in parallel with the gradual breaking of the V$^{2.5+}$-V$^{2.5+}$ bond and formation of trimers.

I. INTRODUCTION

Transition-metal compounds show varieties of electronic properties with spin, charge, and orbital ordering due to electron-electron and electron-lattice interactions of the transition-metal d electrons [1,2]. Among various early transition-metal oxides [3,4], vanadium oxides manifest peculiar electronic structure that can be exploited for various applications. Although V$_2$O$_3$ is a Mott-Hubbard system, the low-temperature antiferromagnetic insulating phase below ∼155K is described by electron-lattice interaction and V $3d$ orbital ordering while the high-temperature paramagnetic metallic phase can still be ascribed with the presence of electron correlation [1,5]. In VO$_2$, the insulating phase is accompanied with the dimerization of V-V atoms below ∼340K [6,7], where V $3d$ orbitals are oriented with electron-electron and electron-lattice interaction. In the LiVO$_2$, trimerization below ∼550K is observed with the orbital induced structural transition and the formation of spin singlets of the triangular lattice [8–10]. The BaV$_{10}$O$_{15}$ undergoes a structural transition accompanied by V trimerization and V $3d$ orbital order at 120 K [11,12]. Recently, the insulating phase below 120 K in BaV$_{10}$O$_{15}$ was reported with V^{2+}-V^{3+} charge ordering and the metallic phase at 300 K with V$^{2.5+}$-V$^{2.5+}$ bond ordering by Yoshino *et al.* [13].

The BaV$_{10}$O$_{15}$ unit cell contains five VO$_6$ octahedra as a boat sharing the edge or face of the octahedron at each

of its four layers. The first layer shares the face with the fourth layer and shares the edge with the second layer where the V trimerization occurs between adjacent layers below 120 K. The V^{2+} and V^{3+} arrangements at the low temperature (75 K) in BaV$_{10}$O$_{15}$ provide V $3d$ orbital ordering analogous to that known in the triangular lattice in LiV^{3+}O$_2$ [9,10]. In the insulating phase of BaV$_{10}$O$_{15}$, V^{2+} and V^{3+} charge ordering is characterized by localized t_{2g} orbitals of d^3 and d^2 site with ferromagnetic coupling between them in the trimer [13–15], which is the case contrary to the spin singlet trimers in LiV^{3+}O$_2$. The Raman studies previously reported on the presence of randomly oriented trimers with decreasing temperature below 220 K [16]. In addition, the splitting of V nuclear magnetic resonance (NMR) spectra indicated the symmetry lowering and no structural transition below 220 K [17]. Further from the NMR and x-ray-diffraction measurements, the phase diagram of BaV$_{10}$O$_{15}$ has shown the high-temperature phase (300–220 K), the intermediate-temperature phase (220–130 K), and the low-temperature phase (below 130 K) [17].

Structural, transport, and optical properties have been studied for BaV$_{10}$O$_{15}$ including the electronic properties only at 75 and 300 K [11–13]. In view of the complicated transport and optical properties across the intermediate-temperature phase [11,16,17], the present work is dedicated to study the electronic properties at 180, 245, and 300 K including the insulating phase (70 K). A band gap of 0.3 eV at the

low-temperature insulating phase was reported from the optical studies [11,18]. With the increase in temperature above 120 K, the resistivity decreases along with a decrease in the positive Seebeck coefficient [19]. Very recently, the surface sensitive scanning photoemission microscopy (SPEM) studies have shown that the metallic domains evolve with temperature above 120 K [20]. As the electronic properties at the surface are different from the bulk due to higher electron correlation and/or charge fluctuation [21], the present hard x-ray photoemission spectroscopy (HAXPES) study would specifically explain the bulk electronic properties of $BaV_{10}O_{15}$ above metal-insulator transition (MIT) and across the intermediate-temperature phase.

The behavior of the electronic transition at intermediate temperature in the correlated metallic phase is extremely important in the context of trimerons reported in Fe_3O_4 [22]. Although the previous HAXPES study by Yoshino *et al.* [13] is based only on the two temperatures, i.e., below and above MIT, the NMR measurement revealed the electronic transition with the $3d$ electrons that couple differently in the three V sites of the triangular lattice across the intermediate-temperature phase [17]. There are localized magnetic V1 and V2-V3 sites with the quasi-one-dimensional itinerant conductivity across the intermediate-temperature range such that the latter leads towards the formation of the trimers below 220 K. Further below MIT, the trimers are ordered with V^{2+}-V^{3+} charge order arrangement in the adjacent layers [13]. The Raman-scattering experiment showed the origin of disorder above MIT due to instability of charge disproportion that is suppressed with long-range ordering below MIT [16]. Looking at the complicated and competitive mechanism of charge ordering/fluctuation in the V $3d$ and their instability with temperature across the intermediate-temperature range, it is extremely important to investigate the nature of the metallic phase with trimers or trimerons by the bulk sensitive HAXPES.

II. METHOD

The single crystals of $BaV_{10}O_{15}$ were prepared as described in the literature [11]. HAXPES measurements were performed at BL09XU of SPring8 [23]. The crystals were fractured under ultrahigh vacuum of 10^{-6} Pa at 300 K. The photoelectrons were excited with photon energy of 7930 eV and collected with the OmicronScienta R4000-10kV analyzer. The pass energy was 200 eV and the total-energy resolution was ~270 meV. The binding energy of each spectrum was calibrated using the Au Fermi edge.

III. RESULTS AND DISCUSSION

Figure 1(a) shows the wide range valence-band HAXPES spectra (step size = 0.05 eV) at 70 K (below MIT at 120 K), 180 K (in the intermediate-temperature phase), 245 K, and 300 K (in the high-temperature phase) normalized with the total intensity. Figure 1(b) shows the valence-band HAXPES spectra near the Fermi edge (step size = 0.02 eV) collected at 70, 180, 245, and 300 K normalized with the height. At the low temperature (70 K), there is no spectral weight at the Fermi level which is consistent with the band gap of 0.3 eV
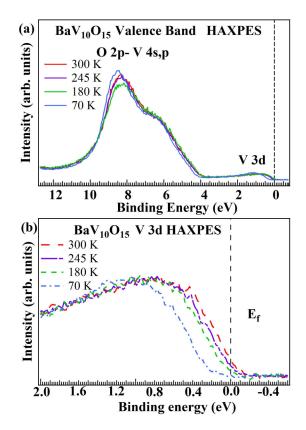

FIG. 1. HAXPES spectra (a) for the entire valence band and (b) HAXPES spectra of $BaV_{10}O_{15}$ near the Fermi-level normalized with its height at 70, 180, 245, and 300 K.

below 120 K accompanied with a structural transition [11,18]. The insulating phase is well established with the V^{2+}-V^{3+} charge ordering and the V trimers between the adjacent layers [13]. On the other hand at 180, 245, and 300 K, the band gap is destroyed and spectral weight appears at the Fermi level. The valence-band HAXPES spectra of the metallic features at 180, 245, and 300 K showed the pseudogap behavior due to the presence of charge fluctuation [13]. Similar features are also seen in other triangular lattice systems [24]. In $BaV_{10}O_{15}$, with decreasing temperature from 300 to 245 K, the spectral weight is shifted away from the Fermi level.

In order to get a detailed understanding of electronic properties above MIT, the V $2p$ HAXPES spectra are collected at 70, 180, 245, and 300 K and are shown in Fig. 2. The V $2p$ HAXPES spectra taken at 75 and 300 K were already explained in the previous paper [13]. The V $2p$ HAXPES spectra at 180 and 245 K including 70 and 300 K are analyzed in this study. The component at the low binding-energy side of the V $2p_{3/2}$ at 300 K is very broad and extends to 512 eV. This is similar to the previous V $2p$ HAXPES results on metallic phase of VO_2 [25], V_2O_3 [26], and $SrVO_3$ [27]. The broadening of the V $2p_{3/2}$ peak is slightly decreased with decrease of temperature from 300 to 180 K. Therefore, it is essential to make a quantitative estimation of the mixed valence from the V $2p$ HAXPES spectra. We adopted six Gaussians (two for the low-energy component of $2p_{3/2}$, two for the high-energy component of $2p_{3/2}$, and two for $2p_{1/2}$) after subtracting the Shirley type background on the V $2p$ for 70, 180, 245, and 300 K (Fig. 2). As the charge-transfer
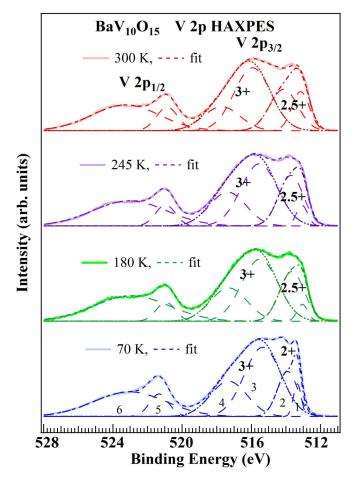
FIG. 2. V $2p$ HAXPES spectra at 70, 180, 245, and 300 K. The fitted results are shown by the dashed curves. The low-energy and high-energy components for V $2p_{3/2}$ are indicated by the dot-dashed and dotted curves, respectively. Six Gaussians are indicated by the large-dashed curves.

TABLE I. Peak position of the low-energy component of V $2p_{3/2}$ obtained from the Gaussians, edge of the low-energy component of V $2p_{3/2}$ shifting from 300 K, $V^{2.5+}/V^{3+}$ or V^{2+}/V^{3+} intensity ratio obtained from the V $2p_{3/2}$ peak fitting, and position of the valence-band edge relative to the Fermi level in $BaV_{10}O_{15}$ at 70, 180, 245, and 300 K.

Temp. (K)	Peak position (eV)	Edge shift from 300 K (eV) ±0.01	Intensity ratio	Position of the valence-band edge relative to the Fermi level (eV) ±0.01
70	513.35	−0.40	0.30	−0.12
180	513.05	−0.10	0.39	0.12
245	513.07	−0.10	0.42	0.15
300	513.15		0.57	0.23

partial breaking of the $V^{2.5+}$-$V^{2.5+}$ bond order with cooling in and above the intermediate-temperature phase. Interestingly, the $V^{2.5+}/V^{3+}$ intensity ratio hardly changes between 245 and 180 K indicating that the trimer formation is almost saturated. It can be consistent with the Raman and NMR studies reporting that the randomly oriented trimers seen with cooling below 220 K were accompanied with an electronic transition [16,17]. Further cooling below MIT, $V^{2.5+}$-$V^{2.5+}$ bond order collapses and transforms towards the insulating V^{2+}-V^{3+} charge order regime. The $V^{2.5+}/V^{3+}$ intensity ratio at 300 K is almost consistent with Yoshino *et al.* [13]. The spectra at 70 K are not the same spectra at 75 K by Yoshino *et al.* [13]. The V^{2+}/V^{3+} intensity ratio is pronounced from 75 to 70 K, consistent with the increase in resistivity and trimers until the Néel order ($T_N = 46$ K) [17].

In the O $1s$ HAXPES, the peak position is not shifted between 300 and 180 K (Fig. 4). In addition, the O $1s$ peak shows much less decrease in the asymmetry (Table II) with decreasing temperature from 300 to 180 K (Fig. 4). If local structural deformation is responsible for the change of V $2p$ between 300 and 180 K, the O $1s$ is expected to change largely due to change of V-O hybridization. As O $1s$ spectral features change only slightly in the opposite direction at the lower binding edge between 300 and 180 K, this indicates that the change between 300 and 180 K is different from that at 120 K. The asymmetry parameter (α) is obtained with the

satellite of the V $2p_{3/2}$ peak in V oxides overlaps the V $2p_{1/2}$ main peak [3], the analysis of the V $2p_{3/2}$ part is useful for such quantification. The low-energy and high-energy components of V $2p_{3/2}$ are located at ~513 eV and ~515 eV, consistent with V^{2+} and V^{3+} components, respectively [28–30]. As the average valence of V in $BaV_{10}O_{15}$ is +2.8, the V $2p_{3/2}$ peak at 70 K is decomposed into V^{2+} and V^{3+} with the V^{2+}-V^{3+} charge ordering while $V^{2.5+}$ and V^{3+} for 180, 245, and 300 K was similarly reported in the recent work [13]. The V^{2+}/V^{3+} intensity ratio is ≈0.30 at 70 K whereas the $V^{2.5+}/V^{3+}$ intensity ratio is ≈0.39, 0.42, and 0.57 at 180, 245, and 300 K, respectively (Table I).

While the high-energy V^{3+} is almost robust, the low-energy component assigned to $V^{2.5+}$ decreases its intensity with cooling from 300 to 180 K. The difference between 300 and 245 K is much larger than that between 245 and 180 K, indicating that there is a valence change between 300 and 245 K. The V $3d$ a_{1g} electron in the $V^{2.5+}$-$V^{2.5+}$ bond order (Fig. 3) contributing to the conductivity decreases its intensity with decreasing temperature below 300 K. The gradual decrease in the $V^{2.5+}/V^{3+}$ intensity ratio would indicate the interplay of the formation of the trimers (random) and the
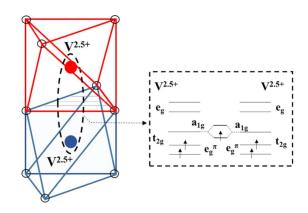

FIG. 3. Schematics of the face sharing V-V octahedral in $BaV_{10}O_{15}$ along with the $V^{2.5+}$-$V^{2.5+}$ bond order of the a_{1g} level [13].
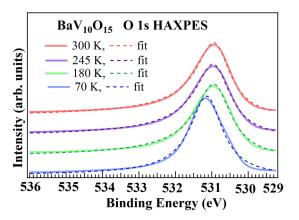
FIG. 4. HAXPES spectra of O 1*s* fitted with the Doniach-Sunjic function at 70, 180, 245, and 300 K.

Doniach-Sunjic function fitted to the O 1*s* spectra at 70, 180, 245, and 300 K, similarly adopted to O 1*s* in $Ba_{1x}Sr_xV_{13}O_{18}$ (Supplemental Material in Ref. [31]). The Doniach-Sunjic profile can be written as $\frac{\Gamma(1-\alpha)}{(\epsilon^2+\gamma^2)^{(1-\alpha)/2}}$ $\cos[\frac{\pi\alpha}{2} + (1 - \alpha)\tan^{-1}(\frac{\epsilon}{\gamma})]$, where ϵ is measured relative to the maximum energy in the absence of lifetime broadening and γ is the width [32]. Although the $V^{2.5+}/V^{3+}$ intensity ratio decreases from 300 to 180 K, the O 1*s* peak is insensitive to the random trimer formation and its partial ordering to the intermediate-temperature phase. The asymmetry for the O 1*s* spectra at 70 K is almost negligible due to the insulating phase.

In Fig. 1(b), there is a decrease of spectral weight above the Fermi level by decreasing temperature below 300 K and it should be related to the decrease in the conducting electrons. Although the valence-band spectra show the pseudogaplike metallic features due to $V^{2.5+}$-V^{3+} charge fluctuation, the increase of pseudogap from 300 to 245 K and further to 180 K is associated with the trimer formation and its partial ordering. With decreasing temperature to 120 K, the trimers are completely ordered in the system and the structural transition is realized. This is exactly consistent with the partial ordering of the trimers with cooling below 200 K reported by Kajita *et al.* [33].

Furthermore, the lower binding-energy edge of the V $2p_{3/2}$ [Fig. 5(a)] follows the shift of the spectral weight near the Fermi edge from 300 to 180 K (Table I) whereas the lower binding-energy edge of the O 1*s* [Fig. 5(b)] behaves oppo-

TABLE II. O 1*s* peak position obtained from the Doniach-Sunjic fitting, the lower binding-energy edge of O 1*s* shifting from 300 K, and O 1*s* asymmetry parameter α in $BaV_{10}O_{15}$ at 70, 180, 245, and 300 K.

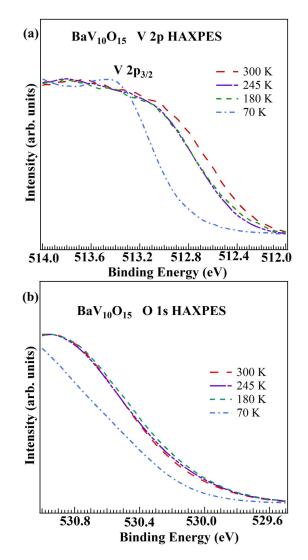| Temp. (K)	Peak position (eV)	Edge shift from 300 K (eV) ±0.01	Asymmetry parameter α
70	531.12	−0.15	0.059
180	530.89	0.05	0.126
245	530.91	0.02	0.134
300	530.89		0.141

FIG. 5. (a) The lower binding-energy edge of V $2p_{3/2}$ HAXPES spectra of $BaV_{10}O_{15}$ at 70, 180, 245, and 300 K. (b) The lower binding-energy edge of O 1*s* HAXPES spectra of $BaV_{10}O_{15}$ at 70, 180, 245, and 300 K.

sitely from 300 to 180 K (Table II). The V $2p$ and O 1*s* spectra exhibit dramatic changes between 70 and 180 K across the MIT indicating that the V-O hybridization and the V-O bond are strongly modified at the MIT. Therefore, electron-lattice interaction is involved in the mechanism of the MIT. On the other hand, the gradual transition between 180 and 300 K shows no change in peak position of O 1*s*. This indicates that the transition is governed by correlated V 3*d* electrons and O 2*p* electrons are not involved. This can be illustrated in the schematics of the face sharing V-V atoms with the V 3*d* a_{1g} electron (Fig. 3). Thus, the charge-orbital change in and above the intermediate phase is purely electronic. The impact of this HAXPES study at temperatures across different transition regimes in $BaV_{10}O_{15}$ would be high, specifically for establishing the electronic properties across the phase transitions from 300 to 180 K using the core and valence level spectra. The electronic transition from 300 to 180 K would involve with the suppression of the V 3*d* a_{1g} bond order of the face sharing $V^{2.5+}$-$V^{2.5+}$ atoms along the *z* axis (Fig. 3). By

further cooling at MIT, the maximum ordering of the trimers would favor maximizing the ferromagnetic order between the V^{2+} and V^{3+} sites, and a structural transition is seen under the V^{2+}-V^{3+} charge order scenario [13]. This induces the insulating phase with the opening of a band gap along the z axis and is consistent to the fact that the Doniach-Sunjic profile would not be useful to fit O $1s$ at 70 K.

Here, it is interesting to compare the trimers in $BaV_{10}O_{15}$ with the trimerons seen in the magnetite (Fe_3O_4). The coexistence of V^{2+}-V^{3+} charge order and trimers is analogous to the case of Fe^{2+}-Fe^{3+} charge order and the trimerons below the Verwey transition [22]. The randomly oriented trimerons become very orderly and lead to an electronic transition by cooling across the intermediate-temperature phase. The trimers in $BaV_{10}O_{15}$ can be viewed as the trimerons in Fe_3O_4. The quasiparticle trimerons exist across the intermediate-temperature phase in $BaV_{10}O_{15}$. Further cooling across 120 K, the splitting of the V^{2+} and V^{3+} sites and ordering of the trimerons lead to the structural transition [13].

IV. CONCLUSION

The electronic properties at 180 K in the intermediate-temperature phase and at 245 K in the high-temperature phase in $BaV_{10}O_{15}$ have been investigated along with the electronic properties at 70 and 300 K both by core and valence-band hard-x-ray photoemission spectroscopies. In going from 300 to 245 K, the $V^{2.5+}$/V^{3+} ratio decreases and the spectral weight moves away from the Fermi level consistent with trimer formation and partial ordering. The lower binding energy edge of V $2p$ shifts consistent with the shift of the spectral weight near the Fermi edge while the binding energy of O $1s$ does not change from 300 to 180 K. There is interplay of the trimers (random) and metallic contribution across 220 K, which is electronic in nature. The pseudogap behavior is present above MIT, in the intermediate-temperature phase, and in the high-temperature phase due to the $V^{2.5+}$-V^{3+} charge fluctuation. The magnitude of the pseudogap increases from 300 to 180 K in parallel with the formation of trimers.

[1] M. Imada, Y. Tokura, and A. Fujimori, Rev. Mod. Phys. **70**, 1039 (1998).

[2] D. I. Khomskii, *Transition Metal Compounds* (Cambridge University Press, Cambridge, UK, 2014).

[3] A. E. Bocquet, T. Mizokawa, K. Morikawa, A. Fujimori, S. R. Barman, K. Maiti, D. D. Sarma, Y. Tokura, and M. Onoda, Phys. Rev. B **53**, 1161 (1996).

[4] S. Dash, T. Kajita, M. Okawa, T. Saitoh, E. Ikenaga, N. L. Saini, T. Katsufuji, and T. Mizokawa, Phys. Rev. B **97**, 165116 (2018).

[5] S. Shin, Y. Tezuka, T. Kinoshita, T. Ishii, T. Kashiwakura, M. Takahashi, and Y. Suda, J. Phys. Soc. Jpn. **64**, 1230 (1995).

[6] S. Shin, S. Suga, M. Taniguchi, M. Fujisawa, H. Kanzaki, A. Fujimori, H. Daimon, Y. Ueda, K. Kosuge, and S. Kachi, Phys. Rev. B **41**, 4993 (1990).

[7] T. C. Koethe, Z. Hu, M. W. Haverkort, C. Schüβler-Langeheine, F. Venturini, N. B. Brookes, O. Tjernberg, W. Reichelt, H. H. Hsieh, H.-J. Lin, C. T. Chen, and L. H. Tjeng, Phys. Rev. Lett. **97**, 116402 (2006).

[8] T. Jin-no, Y. Shimizu, M. Itoh, S. Niitaka, and H. Takagi, Phys. Rev. B **87**, 075135 (2013).

[9] H. F. Pen, J. van den Brink, D. I. Khomskii, and G. A. Sawatzky, Phys. Rev. Lett. **78**, 1323 (1997).

[10] H. F. Pen, L. H. Tjeng, E. Pellegrin, F. M. F. de Groot, G. A. Sawatzky, M. A. van Veenendaal, and C. T. Chen, Phys. Rev. B **55**, 15500 (1997).

[11] T. Kajita, T. Kanzaki, T. Suzuki, J. E. Kim, K. Kato, M. Takata, and T. Katsufuji, Phys. Rev. B **81**, 060405(R) (2010).

[12] K. Takubo, T. Kanzaki, Y. Yamasaki, H. Nakao, Y. Murakami, T. Oguchi, and T. Katsufuji, Phys. Rev. B **86**, 085141 (2012).

[13] T. Yoshino, M. Okawa, T. Kajita, S. Dash, R. Shimoyama, K. Takahashi, Y. Takahashi, R. Takayanagi, T. Saitoh, D. Oot-suki, T. Yoshida, E. Ikenaga, N. L. Saini, T. Katsufuji, and T. Mizokawa, Phys. Rev. B **95**, 075151 (2017).

[14] G. Liu and J. E. Greedan, J. Solid State Chem. **122**, 416 (1996).

[15] C. A. Bridges and J. E. Greedan, J. Solid State Chem. **177**, 1098 (2004).

[16] T. Kanzaki, R. Kubota, and T. Katsufuji, Phys. Rev. B **85**, 144410 (2012).

[17] Y. Shimizu, K. Matsudaira, M. Itoh, T. Kajita, and T. Katsufuji, Phys. Rev. B **84**, 064421 (2011).

[18] A. Nogami, K. Takubo, T. Kajita, M. Hoshino, and T. Katsufuji, Phys. Rev. B **84**, 214442 (2011).

[19] T. Katsufuji, T. Okuda, R. Murata, T. Kanzaki, K. Takayama, and T. Kajita, J. Phys. Soc. Jpn. **85**, 013703 (2016).

[20] T. Yoshino, K. Wakita, E. Paris, A. Barinov, T. Kajita, T. Katsufuji, V. Kandyba, T. Sugimoto, T. Yokoya, N. L. Saini, and T. Mizokawa, Phys. Rev. B **96**, 115161 (2017).

[21] S. Dash, T. Kajita, T. Yoshino, N. L. Saini, T. Katsufuji, and T. Mizokawa, J. Electron Spectrosc. Relat. Phenom. **223**, 11 (2018).

[22] M. S. Senn, J. P. Wright, and J. P. Attfield, Nature (London) **481**, 173 (2012).

[23] E. Ikenaga, M. Kobata, H. Matsuda, T. Sugiyama, H. Daimon, and K. Kobayashi, J. Electron Spectrosc. Relat. Phenom. **190**, 180 (2013).

[24] T. Mizokawa, L. H. Tjeng, P. G. Steeneken, N. B. Brookes, I. Tsukada, T. Yamamoto, and K. Uchinokura, Phys. Rev. B **64**, 115104 (2001).

[25] S. Suga, A. Sekiyama, S. Imada, T. Miyamachi, H. Fujiwara, A. Yamasaki, K. Yoshimura, K. Okada, M. Yabashi, K. Tamasaku, A. Higashiya, and T. Ishikawa, New J. Phys. **11**, 103015 (2009).

[26] G. Panaccione, M. Sacchi, P. Torelli, F. Offi, G. Cautero, R. Sergo, A. Fondacaro, C. Henriquet, S. Huotari, G. Monaco, and L. Paolasini, J. Electron Spectrosc. Relat. Phenom. **156-158**, 64 (2007).

[27] J. Laverock, J. Kuyyalil, B. Chen, R. P. Singh, B. Karlin, J. C. Woicik, G. Balakrishnan, and K. E. Smith, Phys. Rev. B **91**, 165123 (2015).

[28] P. H. Citrin, P. Eisenberger, and D. R. Hamann, Phys. Rev. Lett. **33**, 965 (1974).

[29] G. A. Sawatzky and D. Post, Phys. Rev. B **20**, 1546 (1979).

[30] M. C. Biesinger, L. W. M. Lau, A. R. Gerson, and R. St. C. Smart, Appl. Surf. Sci. **257**, 887 (2010).

[31] S. Dash, M. Okawa, T. Kajita, T. Yoshino, R. Shimoyama, K. Takahashi, Y. Takahashi, R. Takayanagi, T. Saitoh, D. Ootsuki, T. Yoshida, E. Ikenaga, N. L. Saini, T. Katsufuji, and T. Mizokawa, Phys. Rev. B **95**, 195116 (2017).

[32] S. Doniach and M. Sunjic, J. Phys. C **3**, 285 (1970).

[33] T. Kajita, Ph.D. thesis, Waseda University, 2017.